North Atlantic Potential Vorticity and Its Relation to the General Circulation

SCOTT McDOWELL

EG & G Environmental Consultants, Waltham, MA 02254

PETER RHINES AND THOMAS KEFFER

Woods Hole Oceanographic Institution, Woods Hole, MA 02543

(Manuscript received 15 February 1982, in final form 15 July 1982)

ABSTRACT

Maps and sections of the large-scale North Atlantic potential vorticity q are presented. Here q is $fd\rho/dz$, where f is the Coriolis frequency, ρ the potential density and z the vertical coordinate. They bear on the general circulation, and on geostrophic waves, instability and turbulence in many ways; both Eulerian and Lagrangian mean circulations proceed along isostrophes, q = constant, in a zero-dissipation region. In a resting fluid q varies simply as the sine of the latitude, but we show here that the wind-driven circulation reshapes the q-field, creating "bowls" and "plateaus" which allow the flow to cross latitude circles. The implied nature of the western boundary current is very different than in classical frictional theory. The maps show a region of uniform potential vorticity in the wind gyre (σ_θ = 26.5–27.0) which fills the ocean between 15–37°N and 20–80°W. Such regions were prominent features of a circulation theory of Rhines and Young (1982a,b). At deeper levels, and close to surface outcrops of the density layers, the isostrophes are "open," extending over a vast latitude range in mid-ocean. They provide flow paths, for example, which connect the Labrador Sea and the subtropical deep ocean without the need of dissipation of potential vorticity.

The maps of q show where the North Atlantic is susceptible to baroclinic instability. The generalized Rayleigh criterion for instability is satisfied in a large region south of the center of the wind gyre, between 10 and 32°N. This supports the idea that eddy production is a strong feature of the subtropical mid-ocean regions.

1. Review of the dynamics

The equations of motion for large-scale circulation involve nearly geostrophic and hydrostatic balance and consequently, near conservation of the potential vorticity q. The vertical vorticity is singled out because buoyancy twisting terms create only horizontal vorticity at the order of approximation of the equations. Vertical vorticity is created only by stretching and squashing of the basic planetary vortex lines. Thus

$$\frac{Dq}{Dt} = \mathcal{F} - \mathcal{D}, \quad \frac{D\rho}{Dt} = \mathscr{H}, \tag{1.1}$$

where, most generally, $q = (\nabla \times \mathbf{u} + \mathbf{f}) \cdot \nabla\rho/\rho$, $\mathbf{u}$ is the velocity, $|\mathbf{f}| = f_0 + \beta y$ is the Coriolis frequency (a function of y, the north–south coordinate), and ρ is the potential density. D/Dt is the convective time derivative following the horizontal projection of the fluid flow, $\mathcal{F}$ is external forcing (the vertical component of the curl of a mechanical stress), plus a term proportional to the vertical derivative of the buoyancy forcing function. $\mathscr{H}$ is density forcing or diffusive density convergence, and $\mathcal{D}$ is dissipation of q (mechanical or thermal). Defining $\bar{q}$ to be the time-average of q, we have

$$\bar{\mathbf{u}} \cdot \nabla\bar{q} = -\nabla \cdot \overline{\mathbf{u}'q'} + \bar{\mathcal{F}} - \bar{\mathcal{D}}. \tag{1.2}$$

For quasi-geostrophic ocean dynamics the horizontal velocity is nearly nondivergent, and at horizontal scales much larger than NH/f (the Rossby radius, where $N^2 = -g\rho_z/\rho$ and H the depth) the relative vorticity is much smaller than the vortex stretching part of q, provided that the flow is not barotropic. Then

$$\bar{q} \approx \frac{f}{\rho_0}\frac{\partial\rho}{\partial z}, \tag{1.3}$$

and the potential vorticity can be determined from hydrographic measurements of ρ alone.

Unsteady currents, whether free waves, instabilities or geostrophic turbulence, involve interplay between the mean and perturbation fields of q. At one extreme Rossby waves are slight rhythmic undulations of east–west running q-contours [$\bar{\mathbf{u}} = 0$, $\bar{q} = (\beta y + f_0)\bar{\rho}_z/\rho$], while, at another, geostrophic turbulence involves extensive winding and stretching and dissipation of these same contours. Barotropic and baroclinic instabilities are positive-feedback interactions between

0022-3670/82/121417-20$09.00

perturbations in adjacent regions where the mean gradient $\bar{q}$ has opposing senses.

In regions without forcing or dissipation the mean Eulerian circulation $\bar{u}(x, y, z)$ is constrained to follow geostrophic contours ("isostrophes"), q = constant, lying within potential density surfaces. Eddies, through $\overline{q'\mathbf{u}'}$ can drive $\bar{\mathbf{u}}$ across $\bar{q}$ contours as in eddy-resolving numerical models of the circulation (see Rhines and Holland, 1979).

a. q-geometry

In linearized models of the circulation $\bar{q} \propto \beta y$, so that no free flow is possible at all if meridional boundaries block the east–west running contours. Instead, all the Sverdrup transport is confined to the uppermost density layer which communicates directly with the external forcing $\mathcal{F}$. The familiar cycle of potential vorticity input in mid-ocean, followed by dissipation when the fluid parcel reaches the western boundary current, produces a steady flow across $\bar{q}$-contours.

b. Islands of $\bar{q}$

The failure of the above models to predict the vertical structure of the velocity indicates that the ocean circulation is nonlinear (or possibly diffusive). Modification of the $\bar{q}$-contours by the flow itself can allow the interior fluid to move meridionally. As a result fluid could circulate about an entire gyre without feeling external stresses or suffering dissipation near the western boundary. In a vertically integrated sense, dissipation must still occur to balance the integrated wind curl, but this dissipation could occur in a small fraction of the water column, and western boundary currents could then be largely inertial rather than dissipative.

The latter view, that the bulk of the wind circulation involves free conservative flow about islands of $\bar{q}$, rather than a cyclic trade-off between wind forcing and boundary current dissipation, was developed in theoretical work of Rhines and Young (1982a,b). Here we present relevant observations in the North Atlantic. It is consistent with the use of $\bar{\mathbf{u}} \cdot \nabla \bar{q} = 0$, in a local mid-ocean region, by Stommel and Schott (1977) to produce absolute velocity spirals from density data.

The theory, and its predecessors [e.g., the non-diffusive thermohaline circulation theory of Welander (1971)] suggest two essentially different flow regimes, wind-driven and source-sink driven.

In the intense parts of an idealized wind-spun gyre the mean streamlines form nearly closed circuits, upon a ρ surface. Fluid exits and enters the circuit in special regions like surface outcrops and fronts, where eddy processes are active. These may be viewed as a weak "scattering" process which prevents the cyclic travel around the gyre from being perfectly periodic, and, in the large, accounts for the creation, mixing and destruction of water masses.

The crucial feature of the wind-spun gyre, however, is that repeated travel about the nearly closed $\bar{q}$-contours allows the fluid to forget its initial (surface) potential vorticity. Lateral mixing of q occurs, leaving a new and simple q-geometry. In terms of forces, the same events are described as follows. With nearly closed q-contours the fluid at a given depth is very susceptible to weak stresses. With blocked q-contours, as in the linearized theory, a weak wind stress produces a weak flow. But with free paths provided by closed contours, the weak stress exerted by the streamlines above can drive an O(1) circulation. In this way the wind gyre burrows downward to occupy a finite depth interval. The process can continue right to the sea-floor in the most intense parts of the gyre (Rhines and Holland, 1979).

The role of eddies in this wind gyre is particularly ironical. In the fully developed circulation, eddy stresses (e.g., $\overline{u'q'}$) are extremely weak (the flow is nearly free), but the eddies were entirely responsible for spinning up the deeper motion. Thus measurements of weak eddy fluxes "now" may not completely describe their importance to the circulation.

Rhines and Holland (1979) have suggested that vertical momentum flux by eddy form-drag is likely to dominate over lateral momentum flux by Reynolds stress in many circumstances (though not in the vertical-integral momentum balance, unless rough topography is present). This is the eddy flux invoked above. It is interesting that the linear vorticity balance

$$\beta \bar{v} = f \bar{w}_z \tag{1.4a}$$

incorporates this vertical eddy stress (but not lateral stress) through eddy contributions to $\bar{w}$; the eddy fluxes appear explicitly in the density equation

$$\bar{\rho}_z \bar{w} + \bar{\mathbf{u}} \cdot \nabla_h \bar{\rho} = -\overline{w'\rho'_z} - \nabla_h \cdot \overline{\mathbf{u}'\rho'} + \bar{\mathscr{R}}, \tag{1.4b}$$

where ∇_h is the horizontal gradient. The second term on the right-hand side (RHS) corresponds to the geostrophic mixing of potential vorticity (and to form drag) while the first RHS term is dominated by small-scale turbulent mixing [it is smaller, (order Rossby number) than the second, if only geostrophic eddies occur]. The contour-flow equations

$$\bar{\mathbf{u}} \cdot \nabla \bar{q} = 0 \quad \bar{\mathbf{u}} \cdot \nabla \bar{\rho} = 0 \tag{1.5}$$

are less general than (1.4), and assume the RHS of (1.4b) vanishes. Prognostic and diagnostic theories using (1.4) (e.g., Behringer, 1972; Rattray and Dworski, 1978) will be more general than those restricting attention to (1.5).

c. Expulsion: shelves of q

A second property of wind gyres emerges from detailed consideration of the effect of weak eddies.

Beyond having flow-lines coinciding with q-contours, the theory shows the possibility that $\bar{q}$ = constant within gyres (Rhines and Young, 1982b). The "islands" of q thus become shelves or plateaus, as gradients of q are expelled by eddy fluxes. This result of potential vorticity mixing has recently appeared to a striking degree, in numerical eddy-resolving simulations of Holland.

In the discussion of these points (Rhines and Young, 1982a,b) preliminary North Atlantic data were given in support and are repeated below. The anticyclonic gyres predicted by the theory shift poleward with depth, a familiar feature of the observations.

d. Directly driven and thermohaline flow

We have implied a distinction, in a wind gyre, between regions near the external forcing (where a given ρ = constant surface intersects the mixed layer) on the one hand, and recirculating regimes (which appear in more intense western sides of the oceans) on the other. In mathematical terms, the distinction is between solutions of (4) characterized by sea-surface boundary values propagating *along* (ρ, q) contours, and solutions of (4) in which $q(\psi)$ is determined by eddy momentum flux *across* (ρ, q) contours. Two quantities determine the division between these regions: first, the number of times a fluid particle circulates about the gyre before exiting [which Rhines and Young (1982b) call the "recirculation index"] and, second, the time it takes for a fluid particle to forget its initial potential vorticity. It will be important to resolve both these quantities with observations and theory.

Buoyancy flux across the sea surface causes a rather different form of ocean circulation. The flow may in part involve closed horizontal gyres, but it is the penetration vertically and meridionally through the basically stratified domain that seizes ones attention. Below the directly convecting levels, spreading resumes along the intersections of surfaces of constant $\bar{\rho}$ and constant $\bar{q}$, about the deep ocean. This "open-ended" penetration of flow from source to sink contrasts the nearly closed paths in the wind gyre overhead. Near the outcrops where density surfaces intersect the mixed layer, even the wind-driven circulation may resemble a source-sink flow.

The classical theory of the deep circulation (Stommel and Arons, 1960; Stommel *et al.*, 1958) involves, in the non-diffusive case with isolated sources and sinks, purely zonal flow except in western boundary currents. This is the result of linearizing $\bar{q} \approx \beta y$. With density diffusion and compensating vertical motion to support the thermocline, poleward flow is required in the interior, with attendant boundary currents.

If, as above, we allow the fluid to make major deformation of the density surfaces, meridional pathways of constant q can be found in the ocean interior. Yet, these are still subject to the Sverdrup constraint $\beta \int v dz = 0$ if the bottom is flat and no vertical velocity is invoked at the base of the thermocline. Thus in a flat-bottom ocean a source-sink flow still requires important western boundary currents because of this constraint (unless it is so intense that relative vorticity arises in $\bar{q}$ to allow a "short circuit"). But the available bottom ridges and rises make net meridional flow possible without dissipation or other violation of potential vorticity balance. This was the sense in which Stommel and Arons (1972) used rise topography to allow broad western boundary flows which were inertial rather than dissipative.

2. Observations

Maps of water properties on surfaces of constant potential density (e.g., Reid and Lynn, 1971; Broecker and Ostlund, 1979) have long been valuable in discussion of the general circulation. Behringer (1972) produced maps of q for two isopycnal intervals corresponding roughly to 750–1000 m depth in the South Atlantic, using data from the *Meteor* expedition. These show a clear island of q corresponding to the subtropical gyre, 30–45°S, and provide support for the picture of potential vorticity-conserving recirculating flow (even through western boundary currents). Equatorward of the "island," q is dominated by $f(y)$, and the contours are blocked by continents in both east and west. The corresponding dynamic height fields (750–3000 db and 1000–3000 db) show baroclinic gyres coincident with the island and virtually no baroclinic flow equatorward of the island. Both of these features are in agreement with the expectations based on dynamics. The data were too sparse to establish whether the island was also a plateau, with uniform q.

Here an homogeneous hydrographic data set, largely from the 1957–58 IGY program (Fuglister, 1960), and the Erika Dan sections of 1962, has been chosen to make maps of q for the North Atlantic. The positions of the various IGY sections are shown in Fig. 1. These data have recently been used by McDowell (1982a) to do an analysis of oxygen and salinity on potential density surfaces. We plot a finite-difference form of the large-scale potential vorticity,

$$q = \frac{f \Delta \sigma_\theta}{\Delta p},$$

where f is the Coriolis frequency, $\Delta\sigma_\theta$ the chosen vertical interval of the increment (in parts per thousand) of potential density σ_θ (referenced here to the sea surface), and Δp the thickness in decibars of that σ_θ interval. The maps are given only for depths above about 1100 db (the greatest depth of the σ_θ = 27.6 surface), where σ_θ is a fair estimate of potential den-

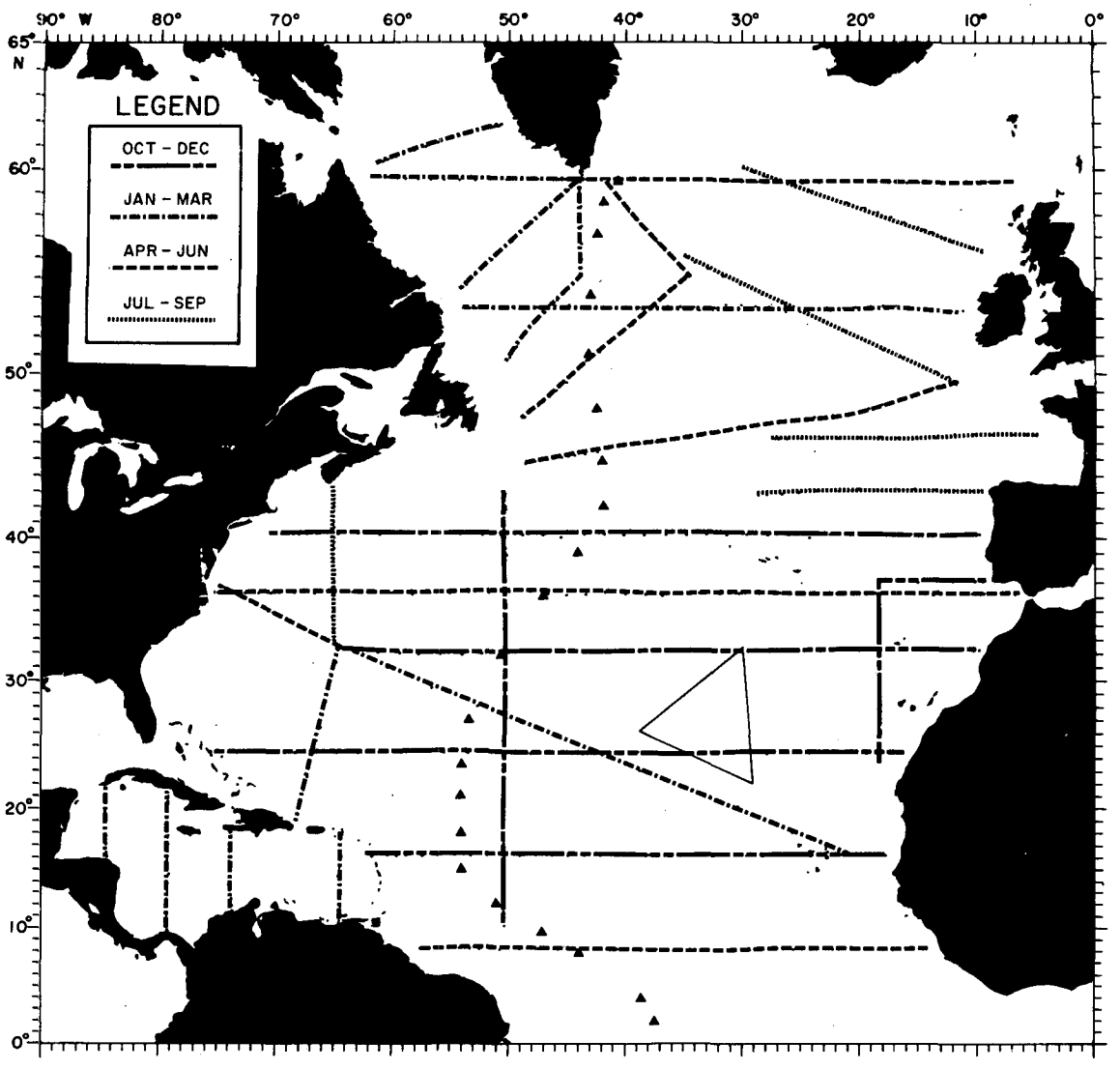

FIG. 1. The distribution of stations used in this study. The dashed lines show the season and cruise tracks of the 1957–58 IGY cruises and the 1962 Erika Dan cruise. GEOSECS Atlantic station positions are indicated by small triangles. The large triangle indicates the region studied by Behringer and Stommel (1980) using the β-spiral method.

sity. The interval $\Delta\sigma_\theta$ is chosen to be large enough to suppress noise in the data, yet small enough to cover a single flow regime. Further refinement of this choice is desirable.

We also describe a meridional section of q calculated from the GEOSECS Atlantic Program (see Fig. 1) which is extended over the full depth range by proper choice of reference levels for potential density. For a given pair of vertically adjacent bottles, the density referenced to their average pressure was calculated. The difference between densities divided by their vertical separation gave the adiabatic density gradient. If there were other bottles within 50 m, then the slope of a least-squares fit of density on depth was used instead. In any case, the estimates of q were then calculated and smoothed using spline fits.

a. Isopycnal topography

The topography of the potential density surfaces $\sigma_\theta = 27.0$ and 27.6 (Figs. 2 and 3), illustrates the character of the wind gyre and the intermediate circulation, respectively. The 27.0 surface shows the bowl shape of the gyre, extending from greater than 800 db northwest of Bermuda, to the sea surface near 45°N. The contours do not show well the narrowness of the Gulf Stream, which is clearer in the augmented data set of Stommel *et al.* (1975). The great east–west extent of the gyre is apparent, but one must be aware that fluid may be entering and exiting the surface at its northern edge through the action of cooling, evaporation and Ekman divergence. It is easy to over-interpret Fig. 2 as being a near representation of the

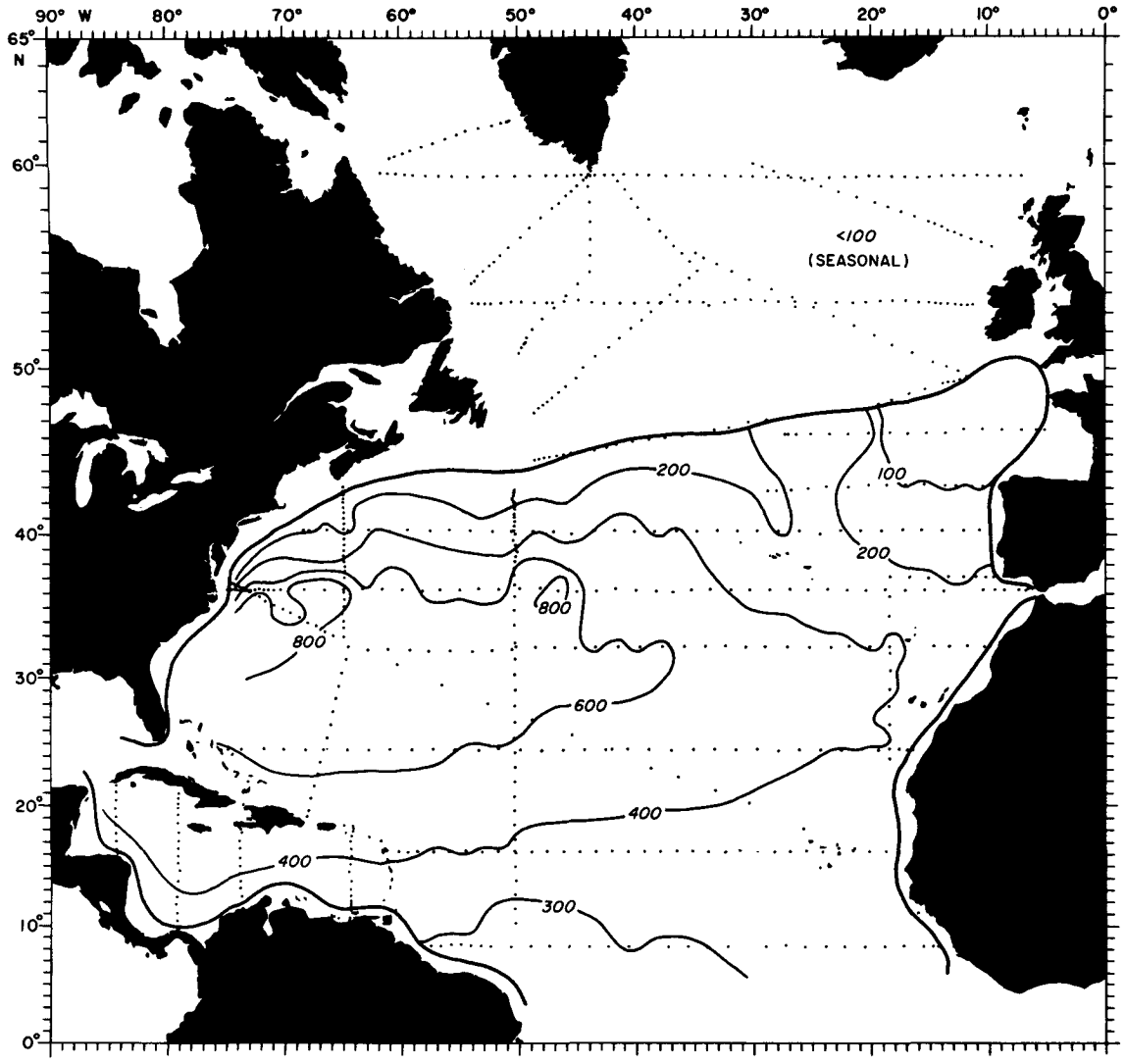

FIG. 2. Pressure (db) on the σ_θ = 27.0 surface. The recirculating gyre is clearly evident, but note that fluid may be exchanged at its northern edge.

streamlines of flow, but the subsequent potential vorticity maps (particularly Fig. 7) will show this to be in error. The problem is that the unknown barotropic mode of circulation may yield mean streamlines that differ substantially from these height contours. It is plausible, instead, to imagine the downward vertical velocity driving the flow "downhill" on the constant density bowl, such that flow crosses height contours at angles which may be large. This sense of w is expected beneath a negative wind curl. The compensating upwelling occurs elsewhere, perhaps in the western boundary current. Correspondence between Fig. 2 and Montgomery and Pollack's (1942) map is quite good, although differing in detail because of their limited data set.

Below, on the 27.6 σ_θ (Fig. 3) surface, the baroclinic signature of the wind gyre has shrunk to a small region of the Sargasso Sea. The isopycnal surface rises steeply in the northwest regions, reaching the sea surface (in this data set) near the mouth of the Labrador Sea. It is close to the surface Reid (1980) used for a study of intermediate waters, and lies above the core of the Mediterranean Water. The isopycnal topography associated with the Gulf Stream, North Atlantic Current, and the top of the Labrador Sea Water is evident. The potential temperature on this surface lies between 11°C near Gibraltar and 3°C far to the northwest, whereas, in the Sargasso Sea, the temperature range is 6 to 7°C.

The intersection of a σ_θ surface with the upper mixed layer is the site of alteration of temperature, salinity and potential vorticity. The "outcrop" curve thus defined is shown in Figs. 2 and 3 for this particular data set. The climatological mean outcrop

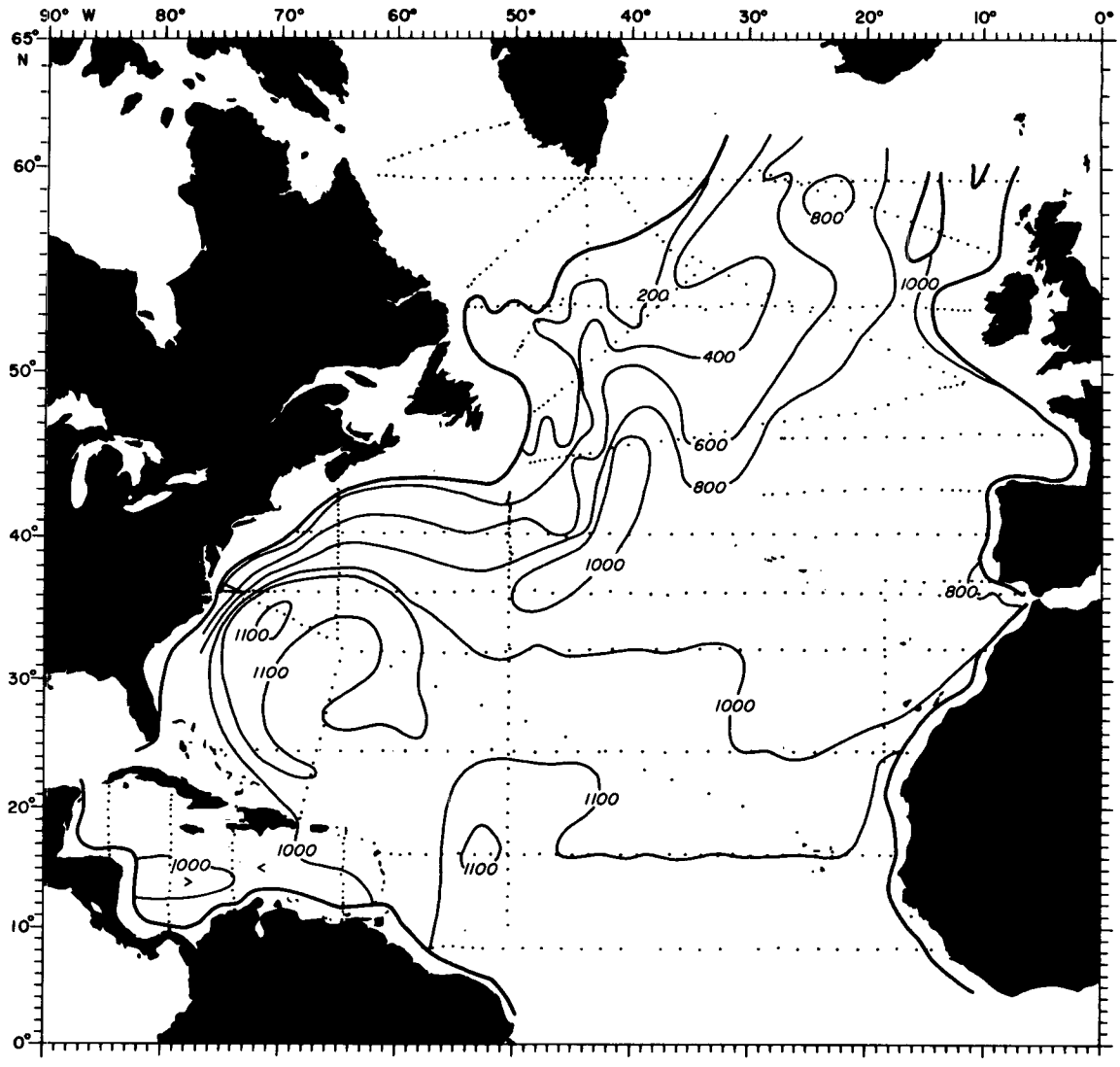

FIG. 3. Pressure (db) on the σ_θ = 27.6 surface. The gyre has shrunk to the northwest. The outcrop region has moved far to the north, outside of the gyre.

curves are dynamically more meaningful, and these are shown in subsequent maps. The position of the outcrop relative to the gyre and to the wind field is important to the dynamics. Lighter-density isopycnals like σ_θ = 26.0 outcrop within the gyre in winter and properties of the downwelled water will strongly reflect atmospheric boundary conditions. Heavier-density isopycnals outcrop outside the wind gyre, putting atmospheric interactions far in the distance, perhaps even in a region where the Ekman-induced vertical velocity is positive. These deeper surfaces have a greater chance of developing a circulation in response to neighboring isopycnals, as outlined above.

b. Potential vorticity maps, σ_θ = 26.0–26.3

This layer lies just below the mixed layer in summertime but is exposed to active convection over much of its area in the wintertime. The geostrophic contours are strongly affected by the flow, with a tendency to close upon themselves and form a gyre (Fig. 4). Because of the inclusion of active forcing at this level within the streamlines, q is not expected to be uniform. Yet in much of the domain, $\bar{\mathbf{u}} \cdot \nabla \bar{q} = 0$ may still apply at the 500 km scale. Also shown in Fig. 4 is the direction and magnitude of the absolute velocity vector at this depth, as estimated by Behringer and Stommel (1980), using the β-spiral method. This method, of course, is a more formal way of determining the direction of q contours on σ_θ surfaces. It, too, depends on eddy fluxes being small at some known pair of depths, but not throughout the water column. The particular estimate that is shown uses a (u_0, v_0) reference velocity at 1000 m of (0.3, 0.1) cm s^{-1}, determined by assuming conservation of q

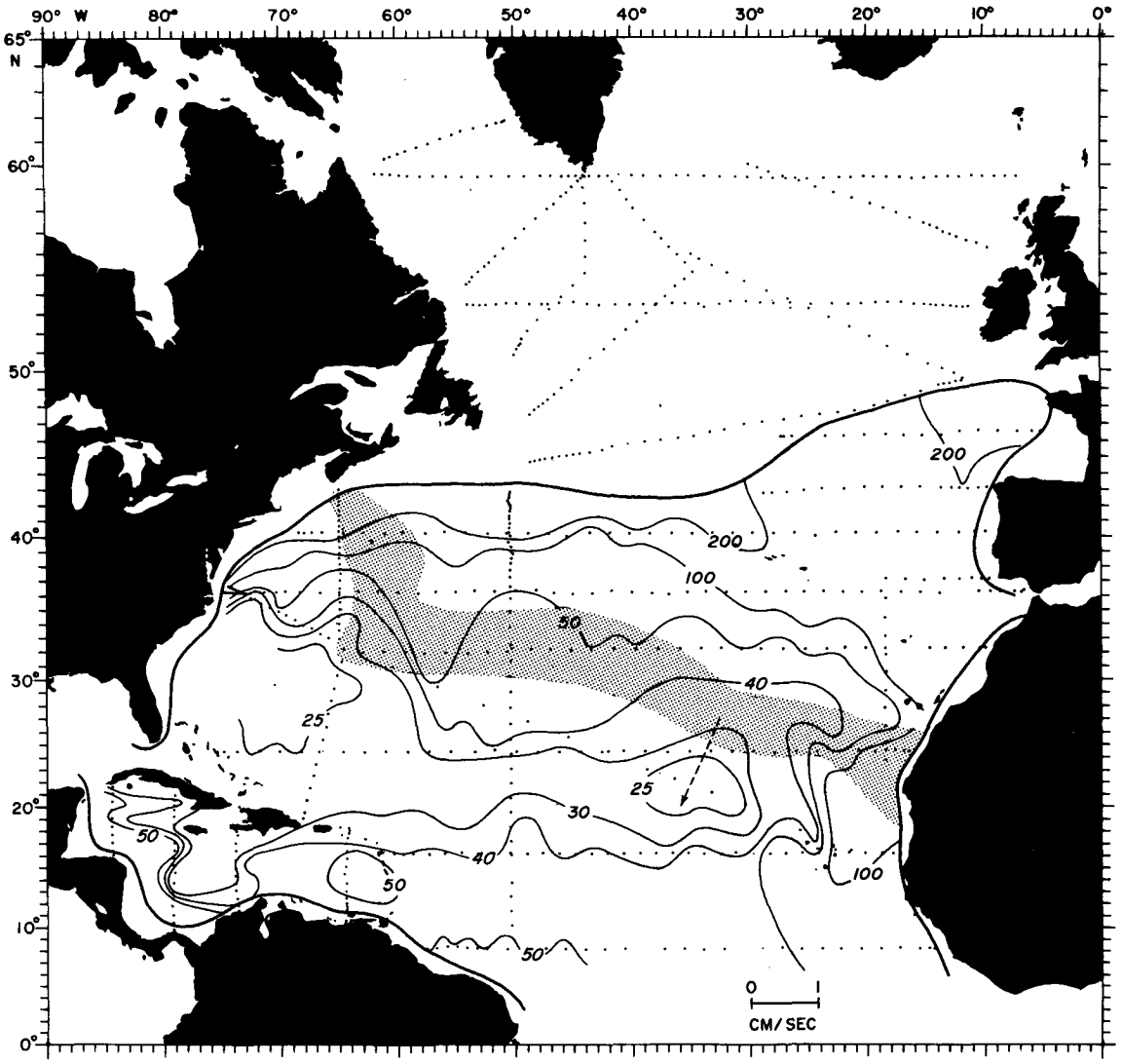

FIG. 4. Potential vorticity (10^{-13} cm^{-1} s^{-1}) computed between the σ_θ = 26.0 and 26.3 surfaces. The bold line represents the outcrop of the 26.0 surface during the observation period. The stippled area lies between the winter outcrops of the two surfaces, determined by the transition to large summer-stratification values where the σ_θ-surface nears the sea surface, and by the large independent data set of Sarmiento *et al.* (1982). The absolute velocity vector estimated by Behringer and Stommel (1980) is shown in the β-spiral region. The geostrophic contours have a tendency to close upon themselves and form a gyre.

below 450 m (see Behringer and Stommel, 1980). The method also requires a strong intersection of constant q and σ_θ surfaces in the interval, so as to avoid an ill-conditioned problem. From these maps of q, the choice 450–1400 m appears to be a good one (see Fig. 7).

Thus, the q-contours give a first approximation to flow paths even at these levels. What can slip by this analysis, however, is intense mixing of σ_θ and q particularly at the Gulf Stream front. Due to poor spatial resolution, our isentropic analysis fails to show any indication of flow around the Grand Banks of Newfoundland into the northern gyre that is evident from maps of dynamic topography. Further understanding of mixing of q and passive tracers in this region is needed to resolve the "two-gyre" controversy (see, Worthington, 1976; Clarke *et al.*, 1980). We emphasize that it is in these areas that the difference between Eulerian mean flow (perhaps related to the average dynamic topography) and Lagrangian mean flow (as seen in water-mass analysis) will be extreme.

The stippled area between the 26.0 and 26.3 winter outcrops is the "window" through which water passes downward from the mixed layer into the interior circulation. On this and succeeding maps we have drawn winter outcrops consistent with both the present IGY data and the large archive of data used by Sarmiento *et al.* (1982). Significant differences were observed

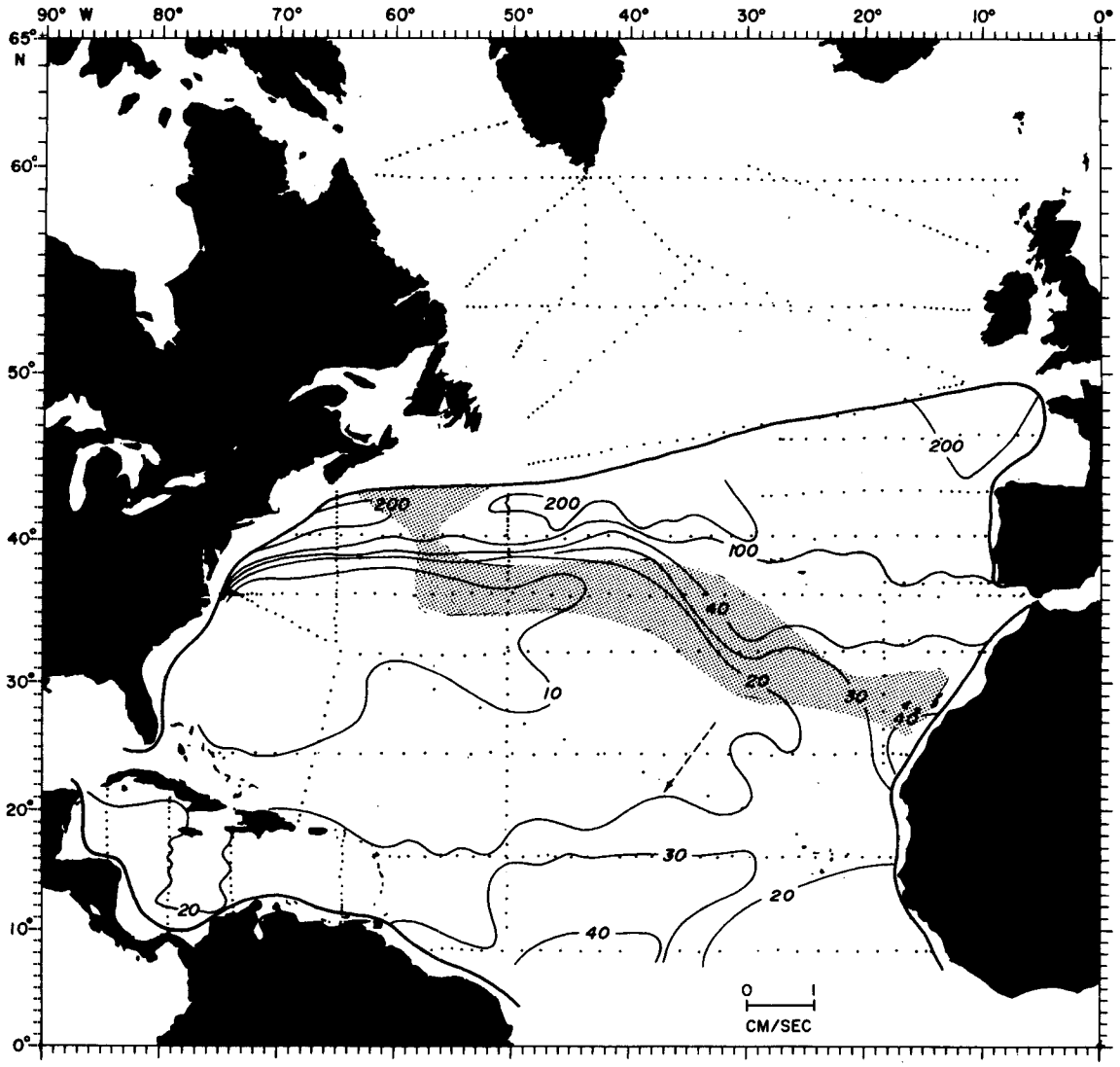

FIG. 5. Potential vorticity between the σ_θ = 26.3 and 26.5 surfaces. Other features as in Fig. 4. The nonlinear control of q contours is clearly evident. Fluid can move great distances meridionally, while conserving its potential vorticity. Note the northward *decrease* in q in the North Equatorial Current region. This marks this area as a likely region of baroclinic instability.

between these outcrop positions and those presented in atlases of surface density but we suspect this is due to nonsynoptic observations. It seems likely that the hydrographic data used here more closely approximate the fields seen by the general circulation. The determination of these windows is made difficult by interannual climate variability. The large "summer" values of q occur north of the stippled outcrop, but such regions are probably not relevant to studies of the subsurface circulation.

Another interesting feature in Fig. 4 is the potential vorticity minimum located at 22°N, 34°W. It is in this region that the high salinity Subtropical Underwater (SUW) is formed by evaporative processes (Worthington, 1976). The SUW increases the vertical density gradient in the upper 150 m of the water column, but immediately below this level and in the range of σ_θ = 26.0–26.3, the gradient is weaker, thus causing q to be a minimum beneath the SUW. The westward homogenization of vorticity is consistent with the advection of salinity and oxygen within this water mass.

c. σ_θ = 26.3–26.5

In this interval situated at the top of the mid-thermocline, the island of q is well formed, showing unambiguously the imprint of the wind gyre between 15 and 40°N (Fig. 5). This extent, of course, is much greater than in the South Atlantic. By nonlinear control of the q-contours, fluid can preserve its potential vorticity while moving through great changes in lat-

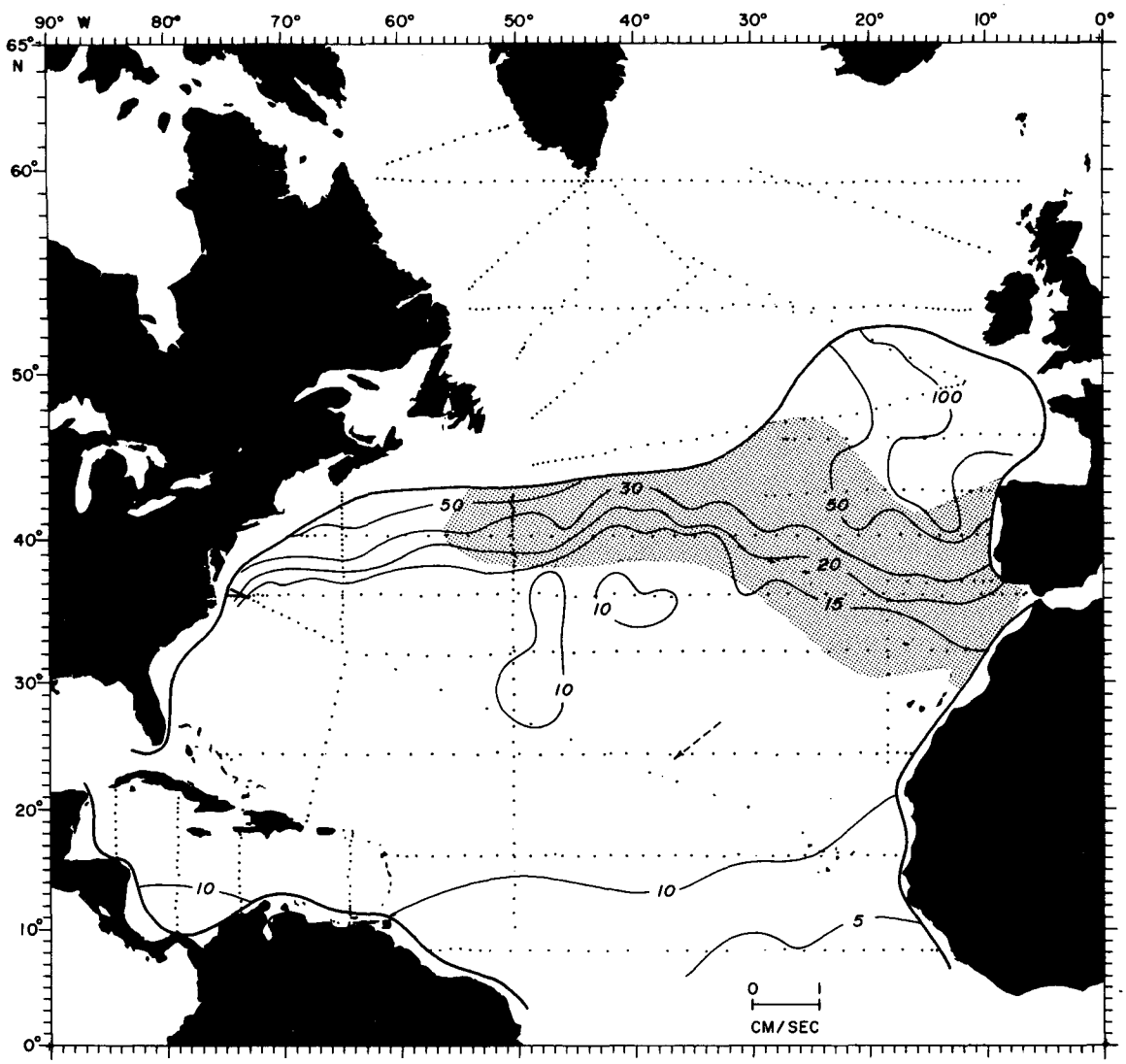

FIG. 6. Potential vorticity between the σ_θ = 26.5 and 27.0 surfaces. A plateau of uniform potential vorticity appears, with steep gradients at its rim (see also Fig. 18).

itude even, possibly, in the western boundary current. The neglect of relative vorticity in the definition of q is probably important only in the Gulf Stream jet. The outcrop window again appears in the q-contours as a boundary between small values and large, the large arising due to the summertime stratification seen on these cruises. On this surface one senses a competition between direct ventilation (down from the outcrop) and recirculation of fluid around the Gulf Stream system.

A striking feature at this level is the northward *decrease* in q ($\partial q/\partial y < 0$) on the equatorward side of the gyre. This large region (15–33°N) is thus most susceptible to baroclinic instability, which is a likely source of eddy activity throughout it. The topic of instability will be discussed in more detail below.

d. σ_θ = *26.5–27.0*

Fig. 6 illustrates a rather thick interval extending from 300 to 800 m depth at 35°N, 70°W and 200 to 500 m depth at 30°N, 35°W. As mentioned above, it characterizes the subtropical wind gyre beneath the typical levels of wintertime mixing.

The gyre is dominated by nearly uniform potential vorticity between 15 and 38°N, across virtually the entire width of the ocean. The depth interval satisfies the conditions Rhines and Young (1982b) used in predicting homogenization of q in the theory. The position of fronts and regions of weak gradient agrees with similar features in the salinity distribution (e.g., Niiler, 1982), and to some extent with the recently input tritium field (Sarmiento *et al.*, 1982). The shape

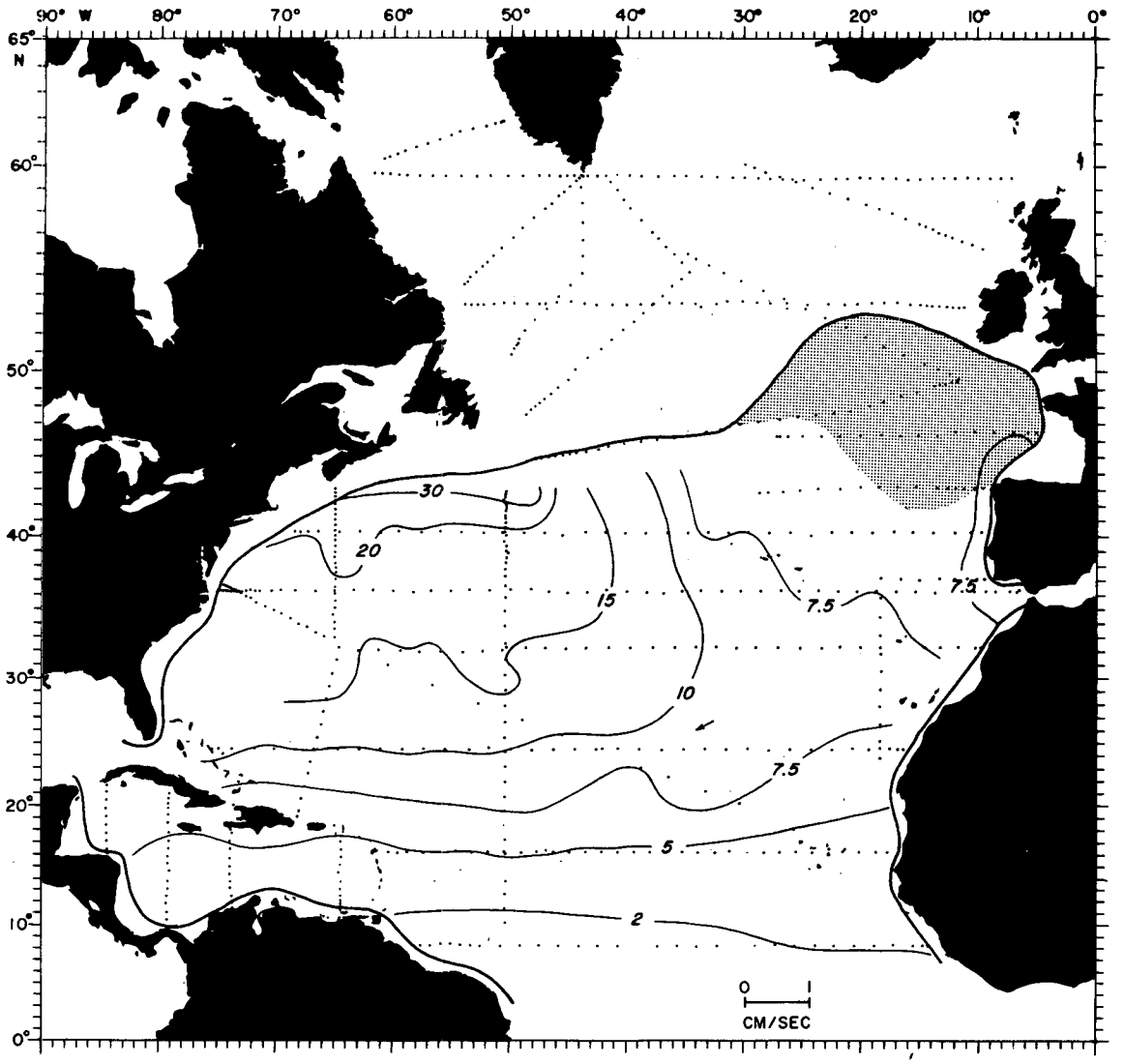

FIG. 7. Potential vorticity between the σ_θ = 27.0 and 27.3 surfaces. The gyre center has moved to the northwest, and strong gradients of q appear again. Note the apparent difference between these idealized flow paths and the corresponding density-height field (Fig. 2).

of the gyre and its abrupt northern and southern boundaries are evident in each of these tracers.

At these levels fluid enters the gyre from the winter-outcrop region and ages as it circulates about (Montgomery, 1938). The process of expulsion of q-gradients may be sufficiently rapid, and the recirculation of fluid about the gyre sufficiently persistent, to cause fluid to forget variations in its input potential vorticity, thus aiding the gyre in becoming homogeneous.

Stommel and Armi (personal communication) have re-examined the β-triangle (see Fig. 1) and have determined that within the interval 200–400 m, the problem becomes ill-conditioned, implying no gradients of q on σ_θ surfaces. The homogenized gyre of q shown in Fig. 6 is clearly in agreement with this result.

e. σ_θ = 27.0–27.3

At the base of the wind gyre we see the "super"-β positive northward gradient of q (Fig. 7) which makes up for the deficit in $\partial q/\partial y$ in the layer above. The geostrophic contours are once again gyre-like with the gyre center receding poleward with depth (also a property of the theoretical models). There is a hint of a small homogenized region in the northwest, between q = 15 and 20, which is more strongly evident in a meridional section (see Fig. 19). Because q-homogenization is not occurring widely at this great depth, we might suspect that the speed of the flow is approaching zero. This is consistent with the increasingly flat isopycnal topography that is found here (see Fig. 2). Fig. 7 might best be viewed as a passive image

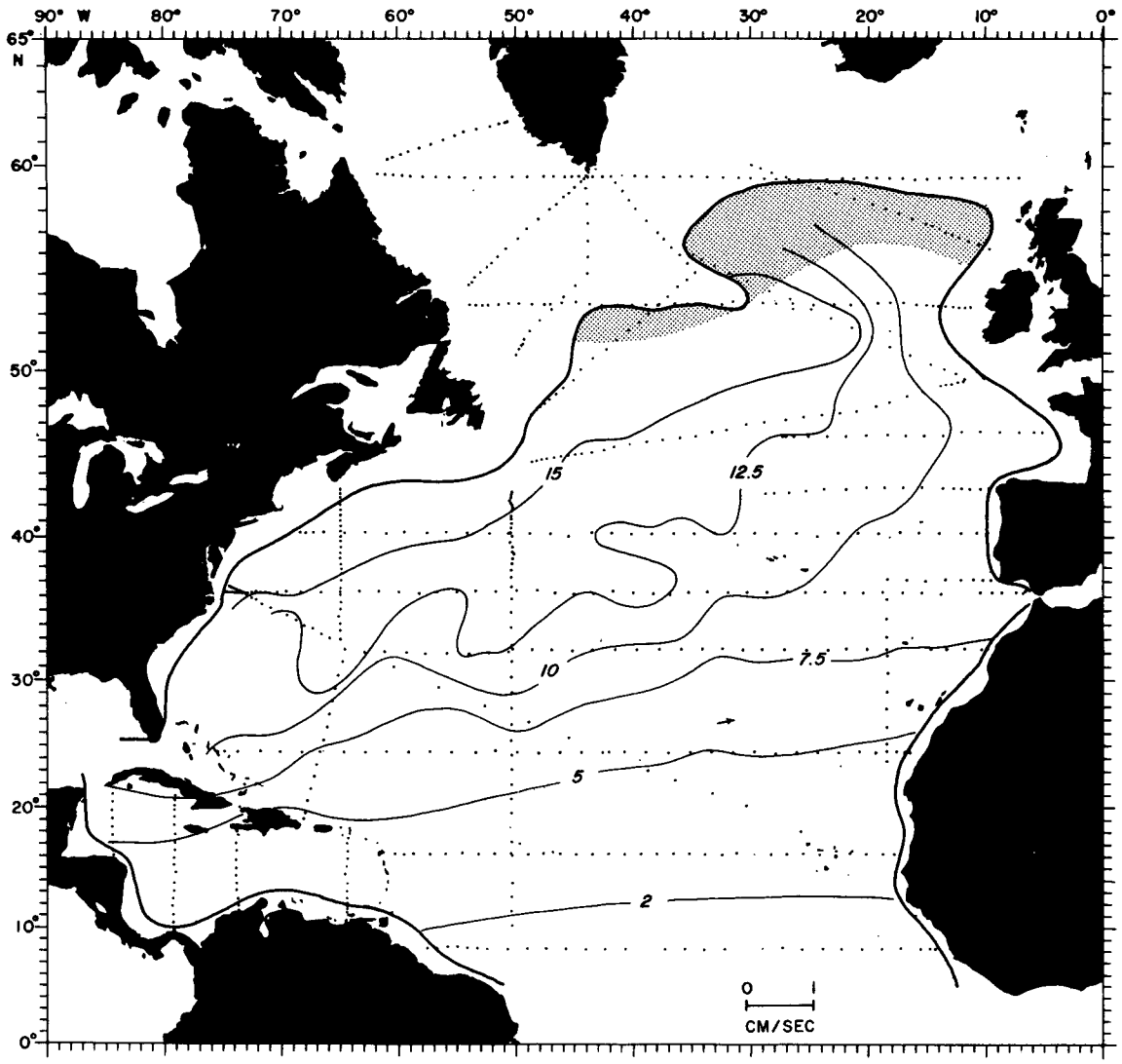

FIG. 8. Potential vorticity between the σ_θ = 27.3 and 27.6 surfaces. The q contours stretch from northeast to southwest, allowing easy communication of fluid between high latitude and the deep subtropical Atlantic.

of the bowl of the active wind gyre, which is situated just above.

The choice of (u_0, v_0) reference velocities by Behringer and Stommel (1980) imply a level of no motion at about 750 m, rather consistent with our suspicion from the q-map at this level. The northeastern part of the domain has quite uniform small values of potential vorticity. McCartney and Talley (1982) trace this water as Sub-polar Mode Water, formed in the West European Basin, presumably south of the zero wind-stress curl line, and then subducted southward along σ_θ = 27.0–27.2.

f. σ_θ = *27.3–27.6*

All of the levels discussed so far show closed, nearly closed, or non-existent geostrophic contours in the wind gyre. The implication is that, at such levels, an inertial western boundary current of a simple form might exist, with fluid entering and exiting at the same potential vorticity. In the 27.3–27.6 density interval (Fig. 8), the geostrophic contours open out to the northeast and have a well-developed gradient. This suggests that we have entered an entirely different flow regime in which there is easy communication of fluid between 25 and 60°N. This is in agreement with water-mass analyses which suggest that water from the Irminger Sea flows along such paths, eventually coming into contact with the warm-water sphere. Farther east the geostrophic contours are suggestive of the extension of Mediterranean water westward across the Atlantic. In the European basin, Mediterranean Water can also flow northward along the boundary while conserving potential vorticity.

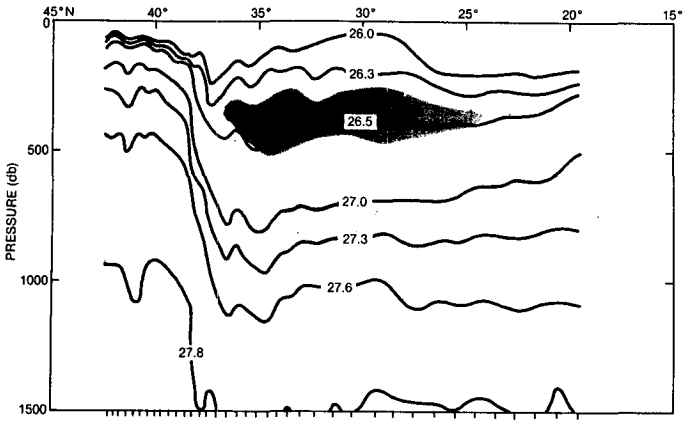

FIG. 9. Meridional section of σ_θ along the 65°W IGY section, with station positions shown at the bottom. Shaded regions indicate the potential vorticity minimum (upper) and maximum (lower) from Fig. 10. The position of the Gulf Stream is evident at 38°N.

This is consistent with the steric height of the 1000 db surface relative to 2000 db that has been presented by Reid (1979).

The potential vorticity field shown in Fig. 8 therefore appears to be a fairly good indicator of preferred flow directions, which agree with those deduced from water-mass analyses. Throughout the subtropical gyre, water parcels are mostly confined to zonal excursions. This is consistent with the discovery of a mesoscale eddy of Mediterranean origin found off the Bahamas (McDowell and Rossby, 1978; McDowell, 1983). The expected trajectory of the eddy is parallel to the large-scale vorticity field, implying conservation of q, but there may have been considerable changes in relative vorticity during this transit. It is interesting to note that the flow direction opposes the weak absolute velocity vector determined by Behringer and Stommel (1980) and shown in Fig. 8. Reversals of flow direction should not be surprising, considering the vertical proximity to the level of no motion. The ambiguity of absolute flow direction is also evident from the steric height maps of Reid (1979).

3. Sections of σ_θ and q

These are sections presented in either the y–z or y–σ_θ plane. They allow examination of the vertical structure of σ_θ and q as well as a more natural view of how isopycnals outcrop and their relation to the latitude of zero wind stress curl.

Two IGY sections are shown, one along 65°W (Figs. 9 and 10) and one along 50°W (Figs. 11 and 12). Also shown is a section from the 1972 GEOSECS cruise (Figs. 13, 14 and 15). All three sections show σ_θ and q in the y–z plane, and the GEOSECS section includes a view of q in the y–σ_θ plane as well.

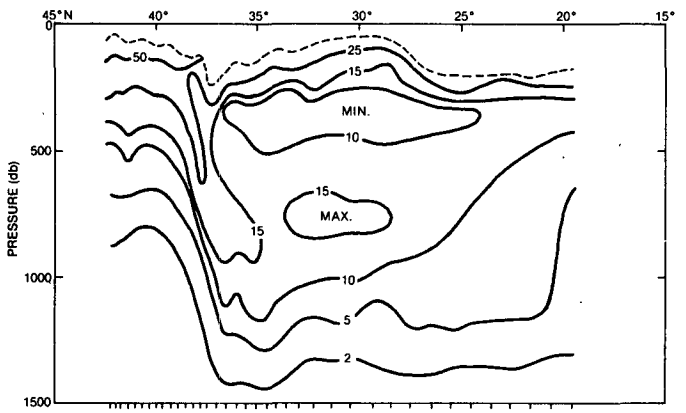

FIG. 10. Meridional section of potential vorticity (10^{-13} cm^{-1} s^{-1}) along the 65°W IGY section. The broad shallow minimum ($q < 10$) is 18°C water, formed by convective cooling at the surface, and subsequently capped off by a seasonal pycnocline. The q maximum at 800 m is the permanent pycnocline.

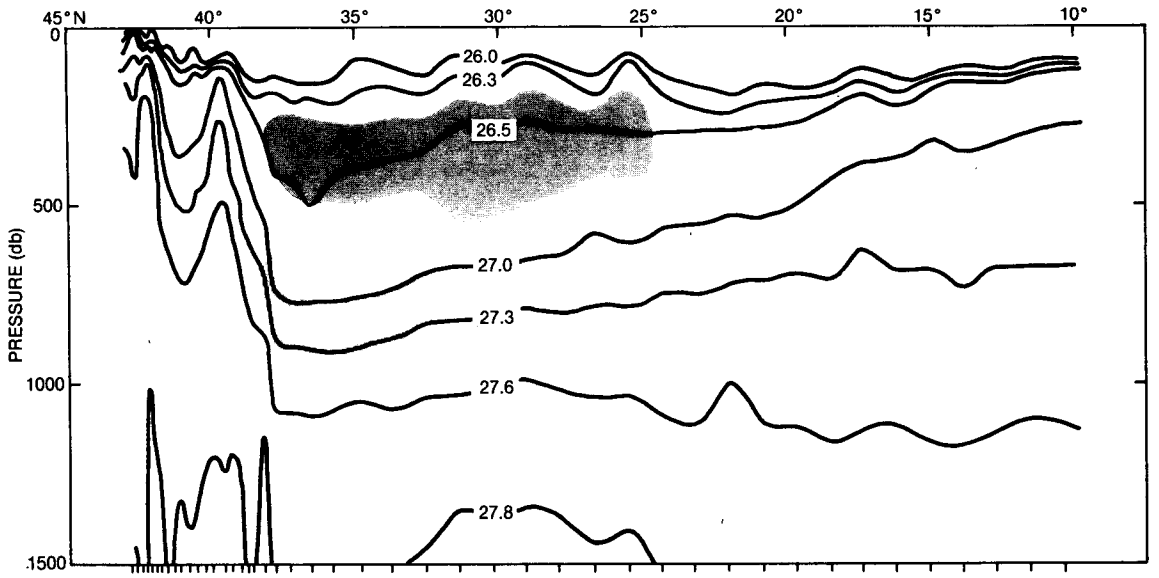

FIG. 11. As in Fig. 9, except 50°W. The Gulf Stream is at 42°N; the doming at 39°N is a cold core eddy. Notice how the σ_θ = 26.3–26.5 and σ_θ = 26.5–27.0 intervals *increase* in thickness to the north of 12°N. The increase is sufficiently strong that it counteracts β, allowing a sign reversal in the gradient of q. See also Fig. 16.

Because the data to the north of 33°N for all three of these sections were taken in the fall, the surface σ_θ outcrops (Figs. 9, 11, 13) have a strong tendency to show the effects of the seasonal thermocline. However, comparison with the maps in Figs. 4 and 6 shows that for all three sections, the winter outcrop of the σ_θ = 26.0 surface is at about 30°N, while the σ_θ = 27.0 surface never outcrops south of 45°N. Because these are the surfaces that outcrop within the gyre, they can be expected to show the effects of Sub-Tropical Mode water formation (Talley and McCartney, 1982). Indeed, the corresponding potential vorticity sections (Figs. 10, 12, 14) show a minimum value at or just below the σ_θ = 26.5 surface. These "pycnostads" are the result of deep convection homogenizing down to 300–400 m, and forming 18°C water. Because the surfaces (σ_θ = 26.5–26.7) all have winter outcrops south of the zero wind-stress curl line, the fluid is advected southward by the implied Sverdrup flow. In the three sections shown, it has reached as far southward as 25°N. Water at these southerly latitudes was probably formed a year or more earlier.

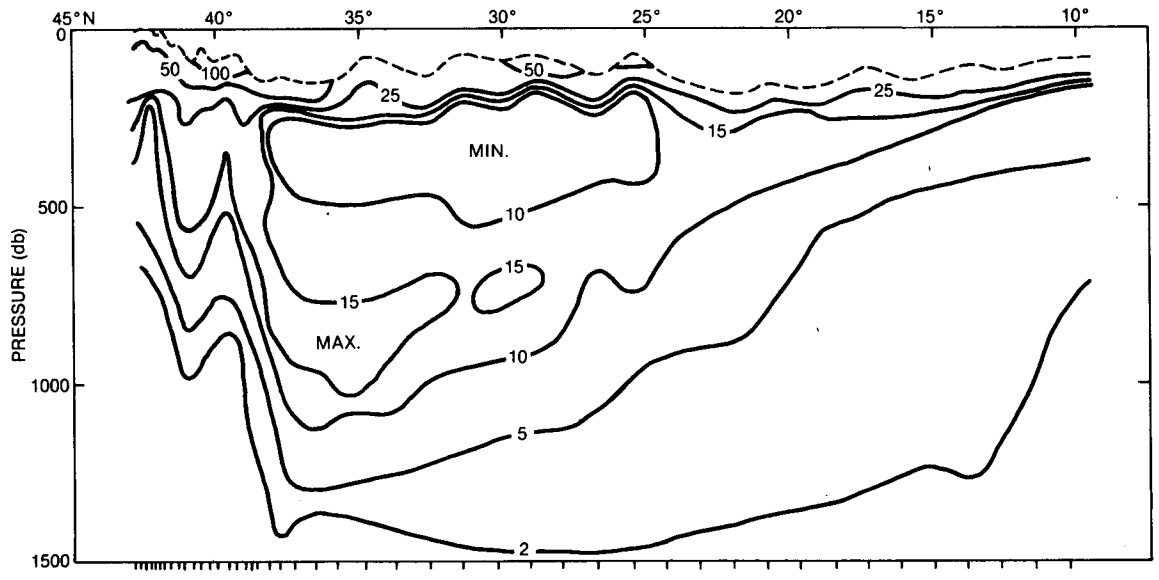

FIG. 12. As in Fig. 10, except 50°W.

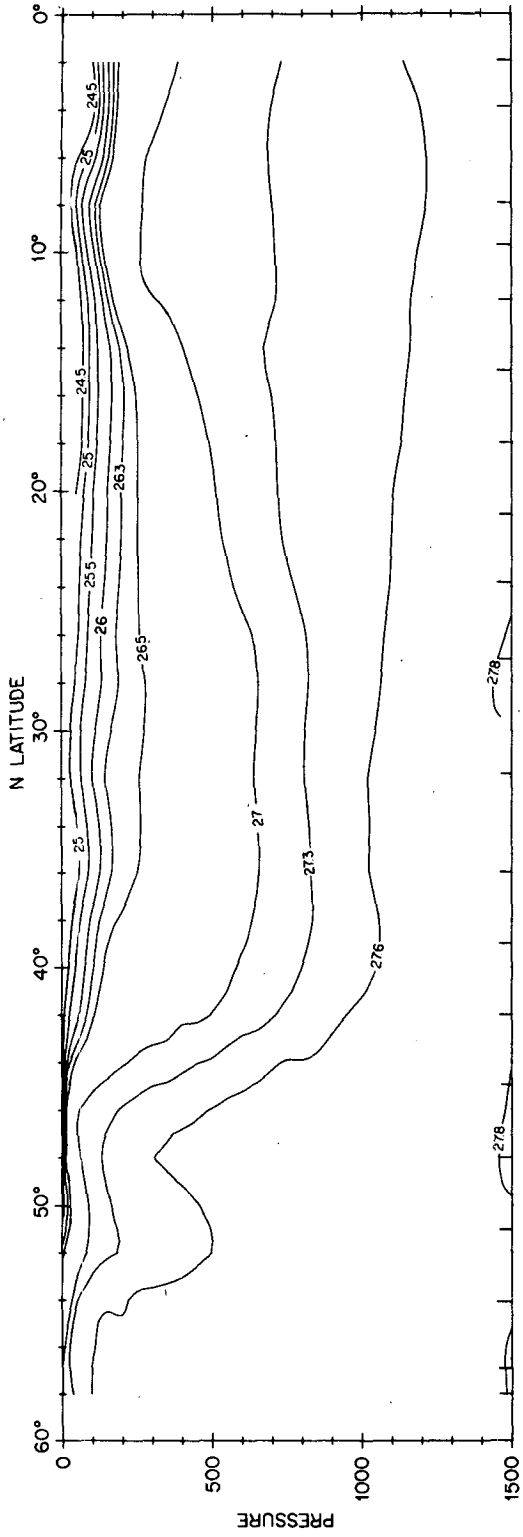

FIG. 13. As in Fig. 9, except the GEOSECS track (see Fig. 1). The Gulf Stream is evident at 42°N. The ridge at 47°N separates the two gyres, with the most northerly front at 51°N being the North Atlantic Current just after separation, offshore of Labrador.

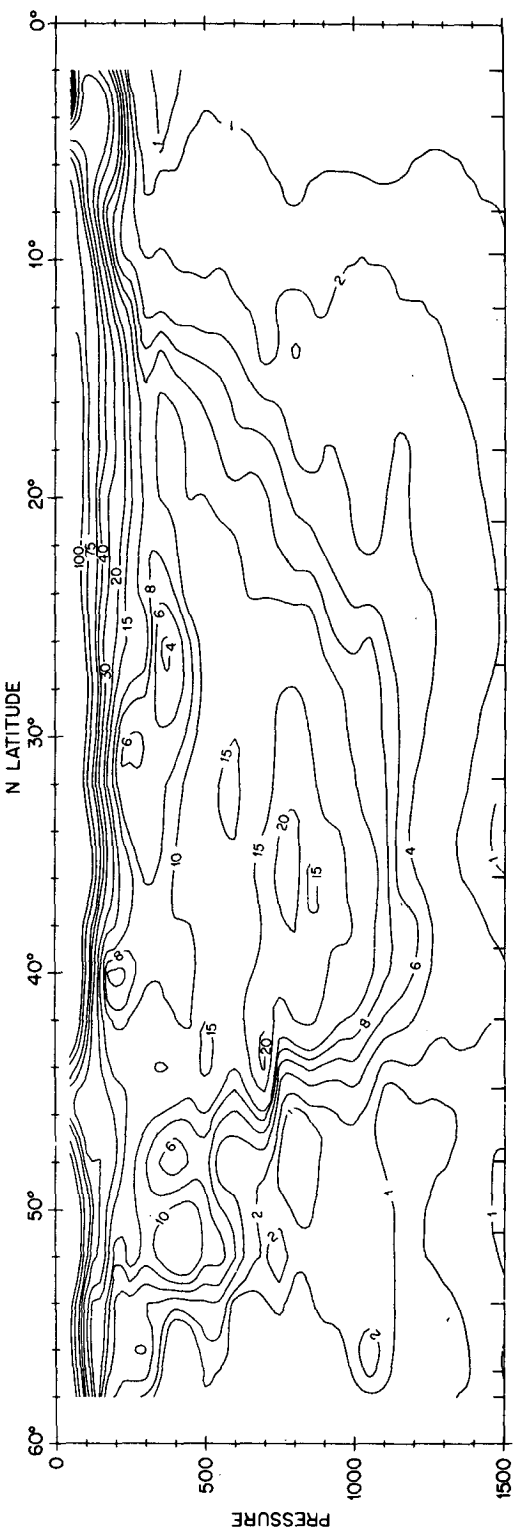

FIG. 14. As in Fig. 10, except the GEOSECS track (see Fig. 1).

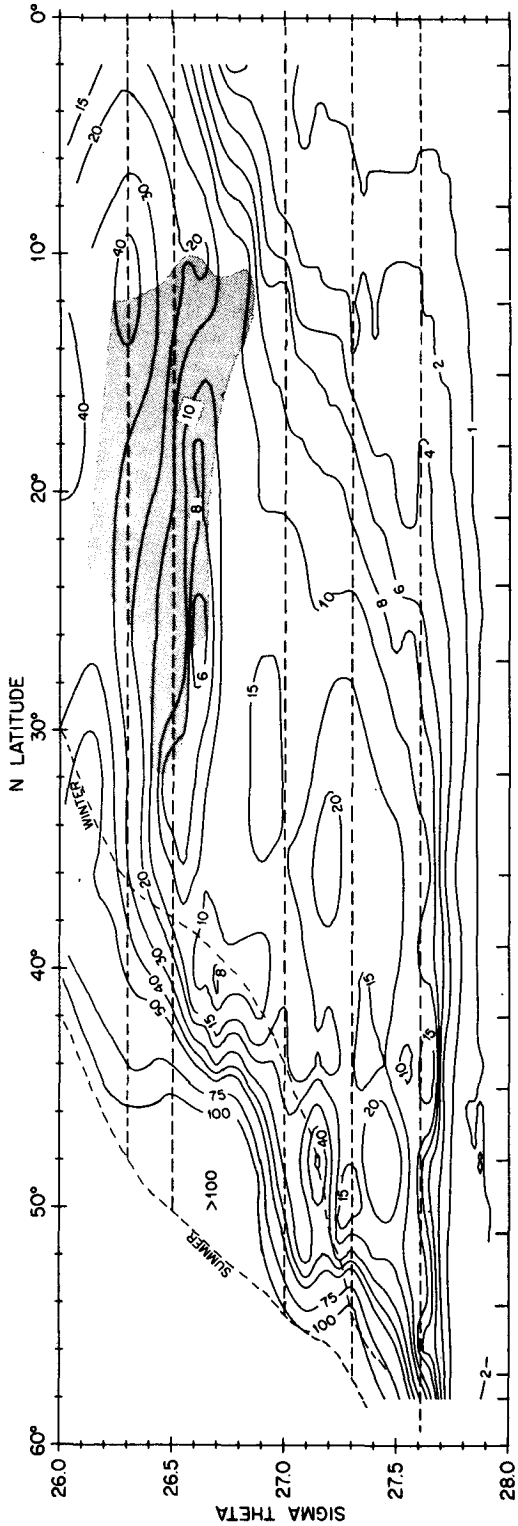

FIG. 15. Potential vorticity (10^{-13} cm^{-1} s^{-1}) from the GEOSECS cruise, plotted against σ_θ. Corresponding with the thickness gradients evident in Fig. 13, regions of constant q on an isopycnal appear as horizontal lines. The North Equatorial Current appears as a region where $\partial q/\partial y < 0$ (shaded) and is a likely site of baroclinic instability. The homogenized gyre appears between 12 and 38°N, centered on σ_θ = 26.8, and ending abruptly with the winter sea-surface outcrop (right-hand dashed line that starts at 30°N, σ_θ = 26.0). The left-hand dashed line is the outcrop at the time of the GEOSECS cruise.

Indeed, the GEOSECS section (Fig. 14) shows a pycnostad reaching downward to nearly 500 m at the unlikely latitude of 26°N. This water is probably a remnant of the unusually severe 1970–71 winter (Talley and Raymer, 1982) that has taken over a year to reach this latitude. Its oxygen concentration of 4.83 mL L^{-1} suggests an age of 12–18 months (Worthington, personal communication).

As the season progresses and the surface waters warm, the low stratification pycnostad becomes capped with a seasonal pycnocline and the surface outcrops move to the north. In these sections the σ_θ = 26.0 surface outcrop has moved 15° of latitude or more. Stommel (1979) has noted similar seasonal migrations of the 20°C isotherm. He hypothesized that the whole intricate system can be modelled as the workings of "Ekman's demon", who selects only winter water to be pumped southward along the isopycnals. Hence only pycnostads and 18°C water, formed far to the north, are observed at 26°N.

Beneath the Sub-Tropical pycnostad lies the permanent pycnocline, and hence, a higher value of q. In these sections, an isolated high is located at about 30 to 37°N at 800 m. Its isolation is due to convergence of isopycnals under the bowl of the wind-spun gyre, as well as the effects of the permanent pycnocline. The north–south asymmetry of the gyre, with its steep poleward edge reflects the poleward thickening of layers in which q is uniform.

Fig. 15 shows q from the GEOSECS data contoured as a function of latitude and σ_θ. The different density intervals used in this study are shown as horizontal lines. The winter outcrop line, estimated from Sarmiento *et al.* (1982), is shown as a dashed line. Because this figure uses a σ_θ coordinate system, regions where q is constant on a density surface appear as horizontal lines. The different dynamical regimes discussed in the dynamics section are clearly evident.

Regions where $\partial q/\partial y < 0$ have been stippled in Fig. 15. These areas are potentially baroclinically unstable (see discussion in the appendix). The North Equatorial Current shows itself as a strong reversal of the potential vorticity gradient at 12–18°N, in the σ_θ = 26.3–26.7 density range (200–350 m). See Keffer (1983) for a discussion of the stability of this region.

The gradient vanishes at approximately σ_θ = 26.8 (300–400 m). This is the depth range where Keffer (1983b) found indications of a critical layer within the North Equatorial Current. Indeed, the profile of $\partial q/\partial y$ displayed in Keffer (1983a) appears to cross zero at 300 m. In linearized theories, critical layers are regions of high eddy heat fluxes. Such a layer could be responsible for eroding away any gradient of q at this level as well.

Just north of the North Equatorial Current lies the homogenized gyre, here most evident on the σ_θ = 26.8 surface. The contours of q are nearly flat, indicating uniform potential vorticity on a density

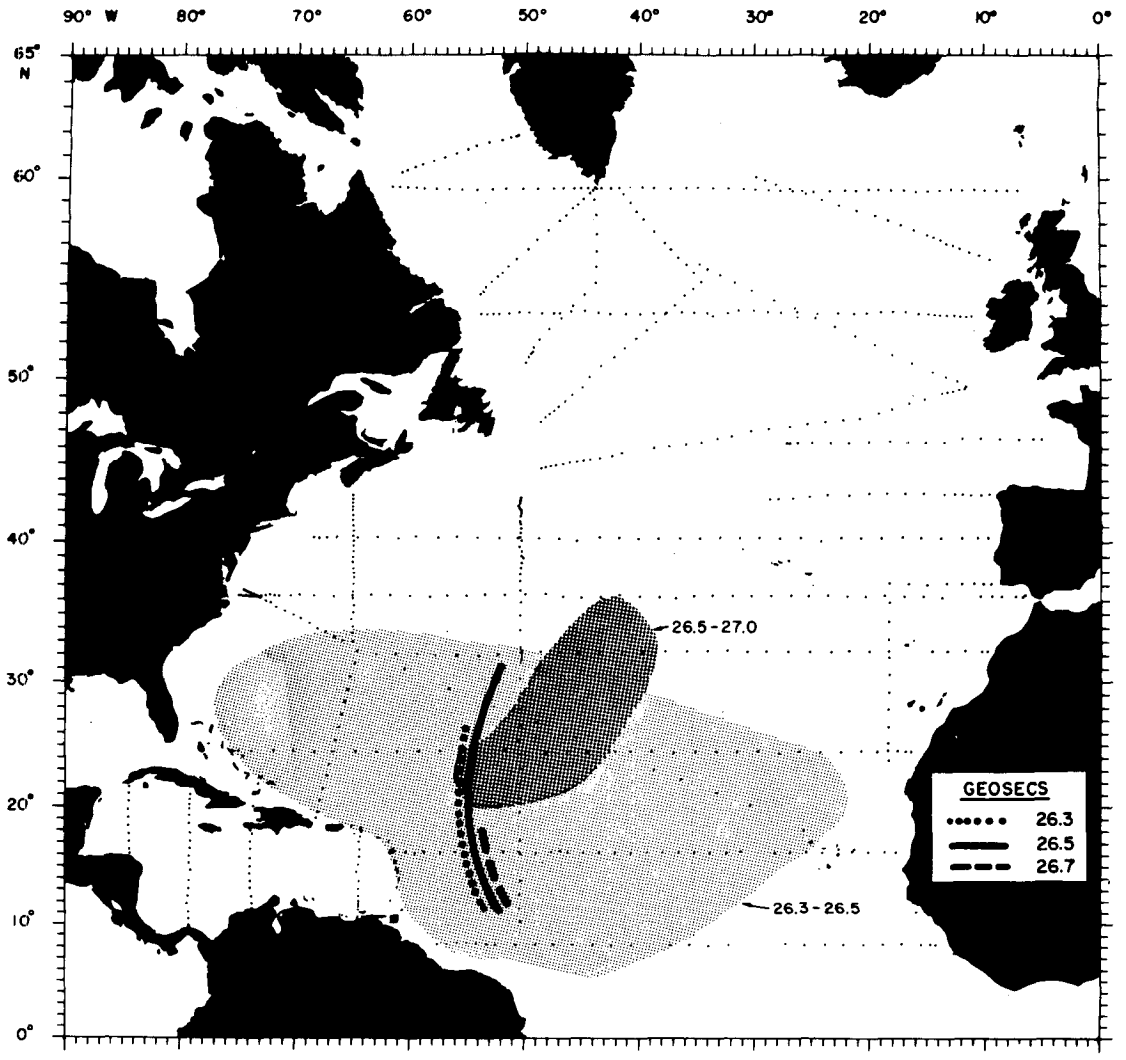

FIG. 16. Geographic regions where the gradient of q reverses direction with depth. These are likely areas of baroclinic instability. The shaded regions were determined from the IGY data, the line segments from the GEOSECS data. Vast sections of the recirculation region may be unstable.

surface. The uniform region ends abruptly at the winter outcrop line at 40°N. Deeper density intervals show much reduced homogenized regions, centered farther to the north, penetrating down to $\sigma_\theta = 27.5$ under more intense regions of the circulation. The gradient of q is everywhere northward outside of the homogenized region.

The region satisfying the necessary conditions for instability, shown in Fig. 16, occupies much of the North Atlantic between 10 and 30°N. This does not guarantee that the circulation is unstable throughout, but the relevant calculations are likely to show growing modes, with growth rate $\approx$ mean current $\times$ Rossby radius in much of the region. It seems timely to calculate not only instability, but also the resulting geostrophic turbulence and wave propagation using these North Atlantic q-fields as a mean state. Strong buoyancy forcing contributes to the instability regions (for example, the 18°C water helping to deepen the minimum of q in mid-gyre). The purely wind-driven set-up of the density field would of itself create such regions, but they might be rather weaker.

4. Meridional scatter plots

The patterns found in the maps of q stand out in transects of raw data from the individual cruises. In Figs. 17–19 we show the data points. The three respective levels show strongly negative $\partial\bar{q}/\partial y$ (σ_θ = 26.3–26.5), nearly uniform q inside the gyre (26.5–27.0), and strongly positive $\partial\bar{q}/\partial y$ below (27.0–27.3). Also, included in Fig. 18 are points calculated from

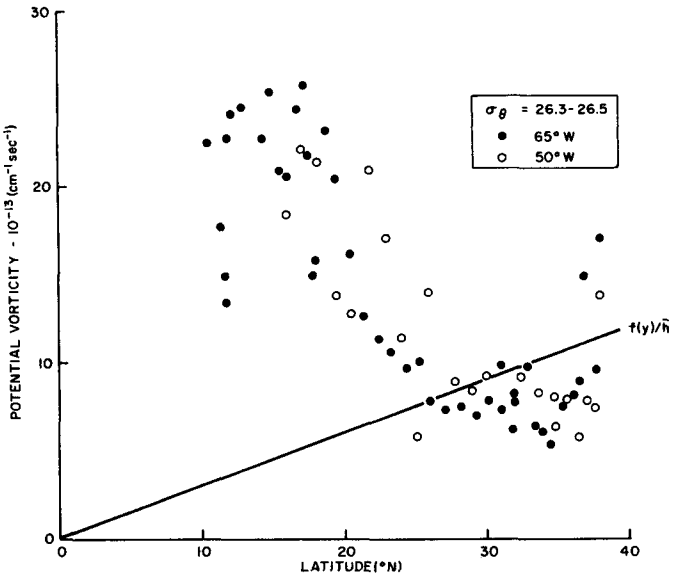

FIG. 17. Potential vorticity computed between the σ_θ = 26.3 and 26.5 surfaces at individual stations along 65 and 50°W (see also Fig. 5). From 15 to 30°N *q decreases* (summarized in Fig. 16). The ambient profile $f(y)/\bar{h}$ is included for comparison.

Montgomery's original (1938) data describing the injection of flow at the outcrops. We have drawn lines $\beta y/\bar{h}$ for comparison, showing that contribution to the q-gradient; $\bar{h}$ is a typical thickness of the respective layers.

5. Conclusion

Fig. 15 summarizes many of our remarks about the circulation. In this meridional section the q-contours are pushed out of the mid-depth wind gyre,

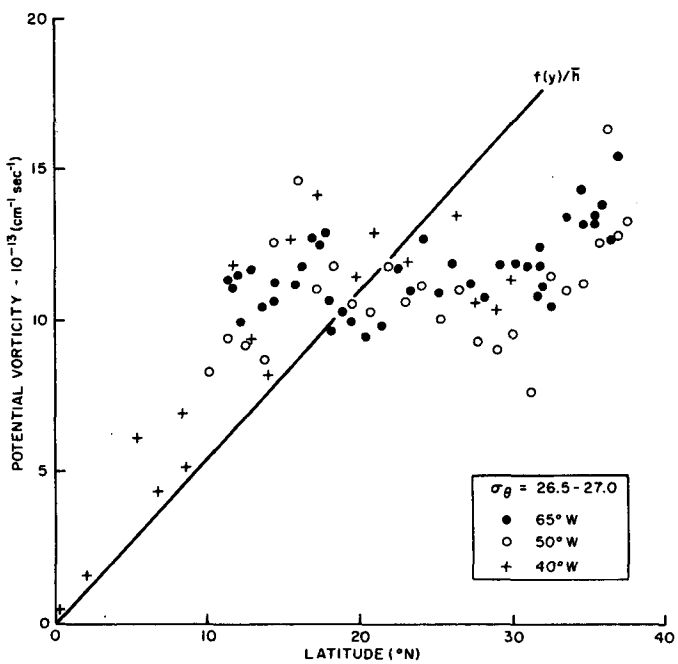

FIG. 18. As in Fig. 17, except σ_θ = 26.5–27.0. This section also includes data along 40°W from Montgomery (1938). A broad plateau of homogenized q extends from 15°N to the south edge of the Gulf Stream at 35°N (see also Fig. 6).

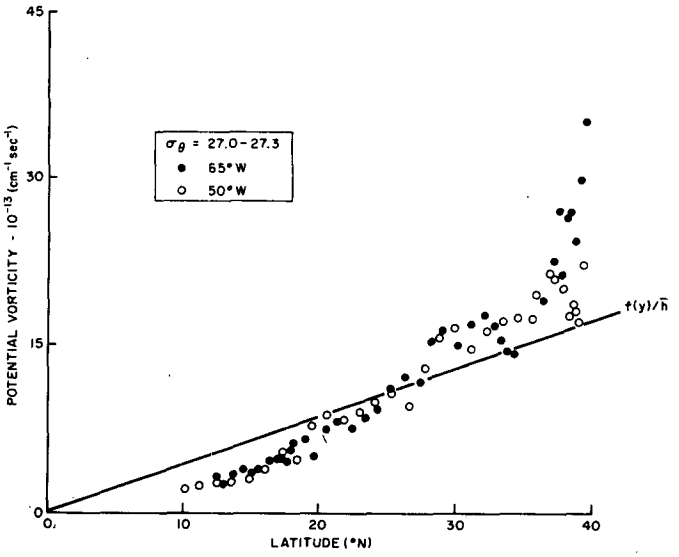

FIG. 19. As in Fig. 17, except σ_θ = 27.0–27.3. The q gradient is "super-β" from 10 to 30°N, to make up for the negative q gradient at shallower depths. There may be a small homogenized region at 32°N.

augmenting the β gradient to the south, and reducing it above (to the point of instability). Below the wind gyre, $\sigma_\theta > 27.7$, q is uniform on σ_θ-levels only because the GEOSECS section happens to follow an isostrophe (see Fig. 8). It is remarkable to see the uniformity of deep ($\sigma_\theta \approx 27.7$–28.0) potential vorticity along this path from 10 to 58°N. Near $\sigma_\theta = 26.5$ we see the effect of local buoyancy forcing in producing a Subtropical Mode-water minimum. North of the winter sea-surface (dashed curve) high values of q reflect seasonal stratification.

Away from boundaries where relative vorticity is known to be significant, the maps of potential vorticity appear to be good indicators of the dynamics that persist within particular density intervals. The transition from the direct wind-driven circulation within gyres to the source-sink regime of the main thermocline is observed in the upper kilometer of the North Atlantic. It will be interesting to see if the downward burrowing of the wind gyre predicted by Rhines and Young (1982b) will be more efficient in other ocean basins where thermohaline circulation is less intense. A secondary factor may be the seasonal fluctuations in the density field that arise from migrations of the isopycnal outcrop regions. Additional analyses will be required to determine whether these fluctuations have a significant impact upon the scales of the planetary gyre and the volume of water which enters the gyre via the Ekman Demon.

The clear definition of the isostrophe field from a small data set suggests a "global" β-spiral calculation in which maps of dynamic height and potential vorticity are merged to form a "most-geostrophic" three-dimensional circulation. The problem is sufficiently overdetermined (by mass and property continuity as well as the isostrophic/isopycnal flow constraint) that regions of violation by higher order eddy-diffusive processes might be clearly identified. See Coats (1981) for related remarks.

Since these maps were produced in mid-1980 (see, e.g., Rhines and Young, 1982a,b) we have become aware of various parallel efforts; Sarmiento *et al.* (1982) show remarkable maps of North Atlantic tritium on σ_θ surfaces and include q-maps based on a large hydrographic data set assembled by Levitus (personal communication). These q-maps are consistent with ours, though differing in some details. Coats (1981) shows that two sections from the North Pacific have uniform potential vorticity through a deep region (down to 1300 m) suggesting that this may characterize the entire wind circulation of the Pacific. It is interesting that the effect of the wind gyre should extend so deep, perhaps because of the lack of strong thermohaline circulation below. D. Olson (personal communication) has looked at the Sargasso Sea potential vorticity and particularly the q-field in Gulf Stream rings. He includes estimates of the relative vorticity. Rhines and Young (1982b) suggest that in homogenized regions eddy potential vorticity should vanish. Their theory in miniature suggests that rapidly rotating rings may try to homogenize their interior q, although interaction with the surface layer and memory of their initial q-distribution may oppose this tendency. R. Watts (personal communication) has made estimates of the relative vorticity in the Gulf Stream, and indeed finds that it tends to compensate for the thickness gradient across the Stream. We recall that in Holland's recent numerical

simulations the separated Gulf Stream jet is completely invisible in a sub-surface potential vorticity map, although it stands out as a strong escarpment in the uppermost layer.

Acknowledgments. A portion of this work was completed while S.M. was a student at the University of Rhode Island, supported by NSF Grant OCE-78-18662. P.R. is supported by NSF Grant OCE-82-23763. T.K. is supported by the Center for Analysis of Marine Systems (at WHOI), which in turn is supported by Exxon and Mobil Foundations, and an anonymous donor.

APPENDIX

Eulerian-Lagrangian Mean Flow Discrepancy and Baroclinic Instability of the Mean Gyre

a. Lagrangian vs Eulerian

The Lagrangian mean circulation is $\bar{\mathbf{u}}^L(t|\mathbf{x}_0, t_0)$, the average velocity of many particles released at independent times t_0 from a single point x_0. The velocities $\bar{\mathbf{u}}^L$ and $\bar{\mathbf{u}}$ may differ significantly. In realistic circulations with eddies $\bar{\mathbf{u}}^L(t)$ behaves eccentrically as the time t after release increases, due to turbulent dispersion of fluid particles. Predictions are available to connect $\bar{\mathbf{u}}$ and $\bar{\mathbf{u}}^L$ only in restricted cases where fluid particles have moved only a small distance compared with the length scale of the mean flow. Rather than being an esoteric distinction, the difference between $\bar{\mathbf{u}}$ and $\bar{\mathbf{u}}^L$ is at the heart of turbulent dispersion of chemical tracers in the sea.

But the extent of violation of geostrophic-contour flow is limited by the strength of the eddies to be typically

$$\bar{\mathbf{u}}^L \cdot \nabla\bar{q}/|\nabla\bar{q}|, \quad \bar{\mathbf{u}} \cdot \nabla\bar{q}/|\nabla\bar{q}| \sim \kappa/L_m ,$$

where κ is the Lagrangian lateral diffusivity due to mesoscale eddies and L_m the lateral scale of variation of mean properties (κ or $\bar{q}$). This says that the eddy-induced mean gyres that do not coincide with q-contours cannot be both strong and large in scale. So, if we are willing to average spatially over these small gyres (perhaps locked to bottom topography) we should recover the simple free circulation

$$\bar{\mathbf{u}} \cdot \nabla\bar{q} = 0, \quad \bar{\mathbf{u}}^L \approx \bar{\mathbf{u}} .$$

The argument from Rhines and Holland (1979) suggests 500 km as a suitable mid-ocean averaging scale in regions where $\bar{\mathbf{u}} = 1$ cm s^{-1}, $\kappa = 10^7$ cm^2 s^{-1}.

b. Waves and instability

Aside from the relevance of $\bar{q}$ to idealized mean flow, perturbations (eddies and waves) see $\nabla\bar{q}$ rather than β as the principal restoring effect. Bottom topography is formally included as a delta-function contribution to $\bar{q}$ at the mean sea floor. Barotropic waves will see predominantly $\bar{q} \approx f/h$ plus contributions from the relative vorticity of the mean flow. For linearized instability to occur, regions of opposing gradients of $\bar{q}$ (projected normal to mean streamlines) must interact. For barotropic instability these regions lie side by side, while for baroclinic instability they lie one over the other.

The result of the Rhines and Young (1982b) theory is that the geostrophic contours must be radically altered from the rest-state, $\bar{q} = \beta y$, if circulation is to exist. This means that baroclinic perturbations will also be radically altered, provided that their vertical scale is comparable with that of $\bar{q}$. The implied theory based on observed $\bar{q}$ has yet to be carried out. But we can remark on the most striking such effect, the baroclinic instability that occurs when the mean potential vorticity gradient changes sign with depth. Many authors (e.g., Gill *et al.*, 1974) have suggested that the equatorward side of the wind gyre is likely to be unstable where the density layers thicken poleward. The present maps delineate the region of this potential "mid-ocean" instability, and that region is extensive. We feel that the eddies observed on the equatorward side of the gyre are likely due to this instability.

The layer-models of Holland give important tests of this idea. He finds that in a small (1000 km × 2000 km) two-layer ocean no mid-ocean instability occurs while in a large (4000 km × 4000 km) three-layer ocean there is a large region of mid-ocean eddy generation. Both models used the same wind stress amplitude, but the larger model has a smaller wind-stress curl. However, the difference occurs largely because the Sverdrup velocity is more intense in a model with a smaller upper-layer thickness h_1. The thickness gradients ∇h_1 can more readily exceed $\beta h_1/f$, allowing $\partial\bar{q}/\partial y$ to become negative in the upper, westward flowing regions. Of course, if a larger ocean had the *same* wind-stress curl, then the Sverdrup transport would be greater as well, further destabilizing the flow. The relevant potential vorticity maps from the two-layer models appeared in Holland and Rhines' (1980) paper.

In conclusion, this discussion suggests that $\bar{q}(x, y, \rho)$ data will provide key reference maps representing idealized flow paths. Violations will occur only where eddies or small-scale vertical mixing are strong enough to drive flow across q-contours. Furthermore, the maps of $\bar{q}$ also provide the background relief for instabilities and waves.

REFERENCES

Behringer, D. W., 1972: Investigations of large scale oceanic circulation patterns using historical hydrographic data. Ph.D. dissertation, University of California, San Diego.

——, and H. Stommel, 1980: The beta spiral in the North Atlantic subtropical gyre. *Deep-Sea Res.*, **27A**, 225–238.

Broecker, S., and H. G. Ostlund, 1979: Property distributions along the σ_θ = 26.8 isopycnal in the Atlantic Ocean. *J. Geophys. Res.*, **84,** 1147–1154.

Clarke, R. A., H. W. Hill, R. F. Reiniger and B. A. Warren, 1980: Current system south and east of the Grand Banks of Newfoundland. *J. Phys. Oceanogr.*, **10,** 25–65.

Coats, D. A., 1981: An estimate of absolute geostrophic velocity from the density field in the northeastern Pacific Ocean. *J. Geophys. Res.*, **86,** 8031–8036.

Fuglister, F. C., 1960: *Atlantic Ocean Atlas of Temperature and Salinity Profiles and Data from the International Geophysical Year of 1957–1958.* Woods Hole Oceanographic Institution Atlas Series, Vol. 1, 209 pp.

Gill, A. E., J. S. A. Green and A. J. Simmons, 1974: Energy partition in the large-scale ocean circulation and the production of mid-ocean eddies. *Deep-Sea Res.*, **21,** 499–528.

Holland, W. R., and P. B. Rhines, 1980: An example of eddy induced ocean circulation. *J. Phys. Oceanogr.*, **10,** 1010–1031.

Keffer, T., 1983a: The baroclinic stability of the Atlantic North Equatorial Current. *J. Phys. Oceanogr.*

——, 1983b: Time-dependent temperature and vorticity balances in the Atlantic North Equatorial Current. *J. Phys. Oceanogr.*, **13** (in press).

McCartney, M. S., and L. D. Talley, 1982: The Subpolar Mode Water of the North Atlantic Ocean. *J. Phys. Oceanogr.*, **12,** 1169–1188.

McDowell, S. E., 1982: Analyses of North Atlantic intermediate waters along isopycnal surfaces and within mesoscale eddies. Ph.D. dissertation, University of Rhode Island.

——, 1983: Anomalous properties of two anticyclonic Sargasso Sea eddies. Submitted to *J. Phys. Oceanogr.*

——, H. T. Rossby, 1978: Mediterranean Water: An intense mesoscale eddy discovered off the Bahamas. *Science,* **202,** 1085–1087.

Montgomery, R. B., 1938: Circulation in upper layers of southern North Atlantic deduced with use of isentropic analysis. *Pap. Phys. Oceanogr. Meteor.*, **6,** No. 2, 55 pp.

——, and M. J. Pollack, 1942: Sigma-*T* surfaces in the Atlantic Ocean. *J. Mar. Res.*, **5,** 21–27.

Niiler, P. P., 1982: The general circulation of the oceans. *Proceedings of the 50th Anniversary Symposium,* Woods Hole Oceanographic Institution (in press).

Rattray, M., and J. G. Dworski, 1978: The effect of bathymetry on the steady baroclinic ocean circulation. *Dyn. Atmos. Oceans,* **2,** 321–339.

Reid, J. L., 1979: On the contribution of the Mediterranean Sea outflow to the Norwegian-Greenland Sea. *Deep-Sea Res.*, **26A,** 1199–1223.

——, 1980: On the mid-depth circulation of the world ocean. *Evolution of Physical Oceanography,* B. A. Warren and C. Wunsch, Eds. The MIT Press, 70–111.

——, and R. J. Lynn, 1971: On the influence of the Norwegian-Greenland and Weddell Seas upon the bottom waters of the Indian and Pacific Oceans. *Deep-Sea Res.*, **18,** 1063–1088.

Rhines, P. B., and W. R. Holland, 1979: A theoretical discussion of eddy-driven mean flows. *Dyn. Atmos. Oceans,* **3,** 289–325.

——, and W. Young, 1982a: A theory of wind-driven ocean circulation, I. Mid-ocean gyres. *J. Mar. Res.*, **40,** Suppl., 559–596.

——, and ——, 1982b: Homogenization of potential vorticity in planetary gyres. *J. Fluid Mech.*, **122,** 347–368.

Sarmiento, J. L., C. G. Rooth and W. Roether, 1982: The North Atlantic tritium distribution in 1972. *J. Geophys. Res.*, **87,** 8047–8056.

Stommel, H., 1979: Determination of water mass properties of water pumped down from the Ekman layer to the geostrophic flow below. *Proc. Nat. Acad. Sci., U.S.*, **76,** 3051–3055.

——, and A. B. Arons, 1960: On the abyssal circulation of the world ocean-II. An idealized model of the circulation pattern and amplitude in ocean basins. *Deep-Sea Res.*, **6,** 217–233.

——, and ——, 1972: On the abyssal circulation of the world ocean-V. The influence of bottom slope on the broadening of inertial boundary currents. *Deep-Sea Res.*, **19,** 707–718.

——, —— and A. J. Faller, 1958: Some examples of stationary planetary flow patterns in bounded basins. *Tellus,* **10,** 179–187.

——, P. Niiler and D. Anati, 1975: Dynamic topography and recirculation of the North Atlantic. *J. Mar. Res.*, **36,** 449–468.

——, and F. Schott, 1977: The beta spiral and the determination of the absolute velocity field from hydrographic station data. *Deep-Sea Res.*, **24,** 325–329.

Talley, L. D., and M. S. McCartney, 1982: Distribution and circulation of Labrador Sea Water. *J. Phys. Oceanogr.*, **12,** 1189–1205.

——, and M. E. Raymer, 1982: Eighteen degree water variability. *J. Mar. Res.*, **40,** Suppl., 757–775.

Welander, P., 1971: Some exact solutions to the equations describing an ideal fluid thermocline. *J. Mar. Res.*, **29,** 60–68.

Worthington, L. V., 1976: On the North Atlantic circulation. *Johns Hopkins Oceanogr. Stud.*, **6,** Johns Hopkins Press.